Available online at www.sciencedirect.com

ScienceDirect

Journal of Sport and Health Science 11 (2022) 696–707

Original article

Exercise attenuates angiotensinII-induced muscle atrophy by targeting PPARγ/miR-29b

Qi Liu [a], Liyang Chen [a], Xuchun Liang [a], Yuqing Cao [a], Xinyue Zhu [a], Siqi Wang [a], Jin Li [a], Juan Gao [b,*], Junjie Xiao [a,b,*]

[a] *Cardiac Regeneration and Ageing Lab, Institute of Cardiovascular Sciences, School of Life Science, Shanghai University, Shanghai 200444, China*
[b] *Shanghai Engineering Research Center of Organ Repair, School of Medicine, Shanghai University, Shanghai 200444, China*

Received 17 February 2021; revised 11 April 2021; accepted 7 May 2021
Available online 8 June 2021

Abstract

Background: Exercise is beneficial for muscle atrophy. Peroxisome proliferator-activated receptor gamma (PPARγ) and microRNA-29b (miR-29b) have been reported to be responsible for angiotensinII (AngII)-induced muscle atrophy. However, it is unclear whether exercise can protect AngII-induced muscle atrophy by targeting PPARγ/miR-29b.

Methods: Skeletal muscle atrophy in both the control group and the run group was established by AngII infusion; after 1 week of exercise training, the mice were sacrificed, and muscle weight was determined. Myofiber size was measured by hematoxylin-eosin and wheat-germ agglutinin staining. Apoptosis was evaluated by terminal deoxynucleotidyl transferase dUTP nick end labeling staining. The expression level of muscle atrogenes, including F-box only protein 32 (FBXO32, also called Atrogin-1) and muscle-specific RING-finger 1 (MuRF-1), the phosphorylation level of protein kinase B (PKB, also called AKT)/forkhead box O3A (FOXO3A)/mammalian target of rapamycin (mTOR) pathway proteins, the expression level of PPARγ and apoptosis-related proteins, including B-cell lymphoma-2 (Bcl-2), Bcl-2-associated X (Bax), cysteine-aspartic acid protease 3 (caspase-3), and cleaved-caspase-3, were determined by western blot. The expression level of miR-29b was checked by reverse-transcription quantitative polymerase chain reaction. A PPARγ inhibitor (T0070907) or adeno-associated virus serotype-8 (AAV8)-mediated miR-29b overexpression was used to demonstrate whether PPARγ activation or miR-29b inhibition mediates the beneficial effects of exercise in AngII-induced muscle atrophy.

Results: Exercise can significantly attenuate AngII-induced muscle atrophy, which is demonstrated by increased skeletal muscle weight, cross-sectional area of myofiber, and activation of AKT/mTOR signaling and by decreased atrogenes expressions and apoptosis. In AngII-induced muscle atrophy mice models, PPARγ was elevated whereas miR-29b was decreased by exercise. The protective effects of exercise in AngII-induced muscle atrophy were inhibited by a PPARγ inhibitor (T0070907) or adeno-associated virus serotype-8 (AAV8)-mediated miR-29b overexpression.

Conclusion: Exercise attenuates AngII-induced muscle atrophy by activation of PPARγ and suppression of miR-29b.

Keywords: AngiotensinII; Exercise; Muscle atrophy; PPARγ; miR-29b

1. Introduction

Heart failure (HF) represents a major cause of morbidity and mortality. HF is accompanied by comorbidities that limit the quality of life and impact prognosis.[1,2] Approximately 30% to 50% of patients with chronic HF have obvious skeletal muscle atrophy,[3,4] which is caused by elevated angiotensinII (AngII) in the circulation.[5–7] Skeletal muscle atrophy with HF can increase the risk of falls, osteoporosis, fractures, cachexia, hospitalizations, and mortality.[8] Except for exercise training,[9,10] there continues to be a lack of effective therapeutic strategies for reversing HF-induced muscle atrophy.

Experimental studies and clinical trials have demonstrated that exercise training can induce major adaptations in skeletal muscle, including increasing muscle mass, promoting muscle regeneration and hypertrophy, reducing inflammation and

Peer review under responsibility of Shanghai University of Sport.
* Corresponding authors.
E-mail addresses: juangao@shu.edu.cn (J. Gao), junjiexiao@shu.edu.cn (J. Xiao).

https://doi.org/10.1016/j.jshs.2021.06.002
Cite this article: Liu Q, Chen L, Liang X, et al. Exercise attenuates angiotensinII-induced muscle atrophy by targeting PPARγ/miR-29b. *J Sport Health Sci* 2022;11:696–707.

reactive oxygen species, and improving mitochondrial function.[11–13] Currently, exercise training is recognized as the only validated therapy for muscle atrophy. However, patients with HF and muscle atrophy are characterized as being exercise-intolerance and as having reduced exercise capacity, which limits the application of exercise therapy.[3,4] Therefore, it is necessary to explore key exercise sensors as novel therapeutic targets for treatment of HF-induced muscle atrophy.

Muscle atrophy is caused by the disturbed homeostasis between protein degradation and protein synthesis. F-box only protein 32 (FBXO32, also called Atrogin-1) and muscle-specific RING-finger 1 (MuRF-1) are 2 important E3-ligases of the ubiquitin-proteasome system. These 2 E3-ligases cause muscle protein degradation, and their expression has been found to increase dramatically during the course of muscle atrophy.[10,14,15] Protein kinase B (PKB, also called AKT)/forkhead box O3A (FOXO3A)/mammalian target of rapamycin (mTOR) is the major pathway that regulates protein synthesis.[10,16,17] Recently, we found that microRNA-29b (miR-29b) was a common regulator of muscle atrophy.[18] We further reported that AngII-induced muscle atrophy via suppression of peroxisome proliferator-activated receptor gamma (PPARγ) was mediated by miR-29b.[19] However, it is unclear whether exercise can protect AngII-induced muscle atrophy by targeting PPARγ/miR-29b.

2. Methods

2.1. Animals

Male C57BL/6J mice (8 weeks old, weighing 20–22 g) were purchased from the Beijing Vital River Laboratory Animal Technology Corporation and maintained in a specific pathogen-free animal center at the School of Life Science at Shanghai University. All procedures with mice followed the guidelines on the use and care of laboratory animals for biomedical research published by the National Institutes of Health (No. 85-23, revised 1996).[18] Our study was approved by the Ethics Committee at Shanghai University.

2.2. Mice exercise model and AngII-induced muscle atrophy model

All mice were randomly separated into 2 experimental groups (total 24 mice, 12 mice per group): Control+AngII group and Run+AngII group. Prior to the experiment, mice assigned to the Run+AngII group were adapted to treadmill running for 1 week, gradually increasing the speed and the duration each day in the following sequence: 5 min (5 m/min) with 0° inclination, 10 min (5 m/min) at a grade of 15°, 20 min (7 m/min) at a grade of 15°, 30 min (9 m/min) at a grade of 15°, 40 min (11 m/min) at a grade of 15°, 50 min (13 m/min) at a grade of 15°, and 60 min (15 m/min) at a grade of 15°.[20,21] After the 1-week treadmill-running habituation, AngII (P1085; Selleck, Houston, TX, USA) was dissolved in a solvent containing 1 × phosphate-buffered saline (PBS, B548117; Sangon, Shanghai, China) and 1 millimole (mM) of acetic acid.[18,19] An osmotic minipump (ALZET Mini-Osmotic Pump Model 2001; ALZET, Cupertino, CA, USA) loaded with the AngII solution was subcutaneously implanted into all mice in both the Control+AngII group and the Run+AngII group. (The skin of the mice was cut between the scapulae to make a small incision; the subcutaneous connective tissues were spread using a hemostat to develop a small pocket under skin; the pump was then inserted into this pocket, and the skin was closed over the incision with a wound clip.) The Model 2001 ALZET miniosmotic pumps are precision drug-delivery tools that infuse at a constant rate in mice (after overnight activation at 37°C, pumps start to deliver 1 μL solutions per hour and will deliver continuously for 7 days). The weight of the mice was about 25 g, on average (10 weeks old); the concentration of the AngII solution was 2.25 mg/mL; accordingly, the AngII solution was released into the mice at a stable dosage of 1.5 μg/kg/min.[18,19] One day after the pump implantation, the Run + AngII group mice started treadmill training at a 15° inclination and a speed of 15 m/min for 60 min/day for 1 week.

To explore whether exercise protects AngII-induced muscle atrophy through activation of PPARγ, a set of mice was randomly divided into 4 groups (total 48 mice, 12 mice per group): Control+Solvent + AngII group; Control + PPARγ inhibitor (T0070907) + AngII group; Run + Solvent + AngII group; and Run+T0070907 + AngII group. Exercise training and AngII infusion were applied to the mice using the same methods described above. PPARγ inhibitor (T0070907, S2871; Selleck) was dissolved in a solvent containing 5% dimethyl sulfoxide (DMSO, D2438; Sigma-Aldrich, St. Louis, MO, USA), 45% polyethylene glycol 300 (PEG300, S6704; Selleck), and 50% sterile water and was intraperitoneally injected (at 1 mg/kg/day) into the mice once daily. The injections lasted 15 days, including 7 days for exercise adaption, 1 day for AngII implantation, plus another 7 days for exercise training. The other 2 parallel control groups were simultaneously injected with the solvent (5% DMSO, 45% PEG300, and 50% sterile water).

To explore whether exercise protects AngII-induced muscle atrophy through miR-29b downregulation, a second set of mice was randomly divided into 4 groups (total 48 mice, 12 mice per group): Control + adeno-associated virus serotype-8 (AAV8)-Control + AngII group; Control + AAV8-miR-29b + AngII group; Run + AAV8-control + AngII group; and Run + AAV8-miR-29b + AngII group. Control AAV8 (AAV8-control) or miR-29b overexpression AAV8 (AAV8-miR-29b) was injected into the gastrocnemius and tibialis anterior at a dose of 10^{11} vector genome (vg) per mouse. AAV8-control and AAV8-miR29b were packaged with 293T cells by the study team. Three weeks after virus injection, exercise training and AngII infusion were applied to mice using the same methods described above.

2.3. Test of grip strength

After exercise training and AngII treatment for 1 week, the grip strength of mice was measured by a digital grip-strength meter (YLS-13; Yiyan Technology, Shanghai, China).[18] First, the value of the force transducer meter was set to 0. The

operator held the tail of the mouse and ensured that the body of mouse was vertical to a metal pull bar. The mouse gripped the metal pull bar symmetrically and tightly while the operator pulled the mouse away at a constant speed to permit the mouse to build up a resistance against it. The force transducer meter recorded the value of grip strength at the point when the mouse released the pull bar. All mice were tested by the same operator to minimize variability. Each mouse was blind-tested 3−5 times with a break of 30 s between tests.

All mice were then sacrificed, and skeletal muscles (gastrocnemius, tibialis anterior, soleus, and extensor digitorum longus) were collected for further analysis.

2.4. Wheat germ agglutinin (WGA) staining

A frozen section of muscle tissue (gastrocnemius and tibialis anterior) was placed in a humid box for 30 min at room temperature, followed by at least 3 washes with 1 × PBS. The frozen section was then fixed with 4% paraformaldehyde (PFA, P6148; Sigma-Aldrich) for 20 min and washed 3 times with PBS. Subsequently, the frozen section was incubated with WGA-conjugates (W11261 or W21404; ThermoFisher, Waltham, MA, USA) and 4, 6-diamidino-2-phenylindole (DAPI, D9542; Sigma-Aldrich) in the dark for 2 h at room temperature. To measure the cross-sectional area of myofibers, images were captured by a Nikon fluorescence microscope (Nikon, Melville, NY, USA), using at least 500 cells and 20 fields of view for each group. The cross-sectional area of myofibers was measured by Image J software (1.50i; NIH, Bethesda, MD, USA).

2.5. Hematoxylin-eosin (HE) staining

Muscle tissue (gastrocnemius and tibialis anterior) was fixed in 4% PFA for 48 h and was then embedded in paraffin (Paraplast Highmelt, 39601095, Leica, Heidelberg, Germany) after dehydration. Muscle tissue sections 5 μm in thickness were stained with hematoxylin (KGA224; KeyGEN, Nanjing, China) staining solution for 5 min, washed with water, and subsequently stained with eosin (KGA224; KeyGEN) staining solution for 10−30 s. Images were captured by Leica microscope (Leica Microsystems CMS, Heidelberg, Germany). Image J software was used to measure cell size and to evaluate the morphological changes in muscle tissue, using at least 500 cells in 20 fields of view for each group.

2.6. Terminal deoxynucleotidyl transferase dUTP Nick End Labeling (TUNEL) staining

Frozen sections of muscle were placed at room temperature for 30 min, washed 3 times with 1 × PBS, fixed with 4% PFA for 20 min at room temperature, and washed with PBS 3 times. The sections were then permeabilized with protease K (V302; Promega, Maidson, WI, USA) in PBS for 10 min at room temperature, washed with PBS 3 times, blocked with 5% bovine serum albumin (BSA, KGY00850; KeyGEN) at room temperature for 2 h, incubated with the DeadEnd Fluorometric TUNEL System (G3250; Promega) at 37˚C for 1 h, and stopped with 2 × saline-sodium citrate (SSC, G329; Promega). The frozen sections were then incubated with WGA-conjugates (W21404; ThermoFisher) and DAPI (D9542; Sigma-Aldrich) in the dark at room temperature for 2 h. Images were captured by a Nikon fluorescence microscope, and the proportion of TUNEL-positive nuclei to total nuclei was measured using Image J software.

2.7. Muscle fiber immunostaining

To determine the muscle fiber types, frozen sections (20 μm) of gastrocnemius was placed in a humid box for 30 min at room temperature, followed by at least 3 PBS washes. Then the frozen section was fixed with 4% PFA for 20 min and washed with PBS 3 times, permeabilized with TritonX-100 (T8787; Sigma-Aldrich) for 20 min, washed with PBS 3 times, and blocked with 5% BSA at room temperature for 2 h. Subsequently, the frozen sections were incubated overnight with the primary antibodies against myosin heavy chain type I (BA-D5; DSHB, Iowa City, IA, USA), myosin heavy chain type IIA (SC-71; DSHB), and myosin heavy chain type IIB (BF-F3; DSHB). The sections were also incubated for 2 h with the corresponding secondary antibodies (Alexa Fluor™ 350 anti-mouse IgG2b for BAD5, A21140; Alexa Fluor™ 488 anti-mouse IgG1 for SC-71, A21121; Alexa Fluor™ 555 anti-mouse IgM for BF-F3, A21426; ThermoFisher). Images were obtained with a confocal microscope (LSM880; Zeiss, Oberkochen, Germany), and the proportions of type I, type IIA, and type IIB muscle fibers to total muscle fibers were measured using Image J software.

2.8. Western blot

Protein samples were extracted from muscle samples of gastrocnemius by using a phosphoprotein isolation kit (KGP9100; KeyGEN). Lysates were centrifuged 12,000 *g* for 10 min at 4˚C, and the supernatants were aliquoted and stored at −80˚C. A Bicinchoninic acid (BCA) Protein Assay kit (T9300A; Takara, Kyoto, Japan) was used to determine the concentration of the protein sample. Equal amounts of protein from the various groups were separated by Sodium dodecyl sulfate-polyacrylamide gel electrophoresis (SDS-PAGE) and transferred to the polyvinylidene fluoride membrane (ISEQ00010; Millipore, Billerica, MA, USA), blocked with 5% BSA, and then incubated with primary antibody. The antibodies used in our study were: PPARγ (A0270; Abclonal, Wuhan, China), AKT (10176-2-AP; Proteintech, Wuhan, China), phospho-AKT (Ser473) (p-AKT (S473), #4058; CST, Danvers, MA, USA), phospho-AKT (Thr308) (p-AKT(T308), #2965; CST), FOXO3A(10849-1-AP; Proteintech), phospho-FOXO3A (Ser253) (p-FOXO3A (S253), #9466; CST), mTOR (#2972; CST), phospho-mTOR (p-mTOR, #2971; CST), p70 Ribosomal Protein S6 Kinase (p70S6K, #9202; CST), phospho-p70S6K (p-p70S6K, #9205; CST), eukaryotic initiation factor 4E (eIF-4E) binding protein 1 (EIF-4EBP1, A1248; Abclonal, Wuhan, China), phospho-EIF-4EBP1 (p-EIF-4EBP1, AP0032; Abclonal), Bcl2 (A19693; Abclonal), Bax (A12009; Abclonal), Caspase-3 (A0214; Abclonal), and

glyceraldehyde-3-phosphate dehydrogenase (GAPDH, AP0063; Bioworld, Nanjing, China).

2.9. RNA isolation followed by reverse-transcription quantitative polymerase chain reaction (RT-qPCR)

Total RNAs were isolated from skeletal muscle tissues of gastrocnemius using RNAiso plus (9109; Takara, Kyoto, Japan) and were reverse-transcribed by a RevertAid first-strand cDNA synthesis kit (K1622; ThermoFisher). qPCR was performed by using SYBR Premix Ex Taq (RR420A; Takara) and the Roche real-time PCR detection system (LightCycler 480 System; Roche, Basel, Switzerland). The bulgeloop miR-29b and 5S ribosomal RNA (5S rRNA) RT and qPCR primer set were obtained from RiboBio (RiboBio, Guangzhou, China). 5S rRNA was used as an internal control and the relative miR-29b level was determined by the $2^{-\triangle\triangle}$CT (cycle threshold) method. The mRNA levels of *myosin heavy chain 1* (*Myh1*), *myosin heavy chain 2* (*Myh2*), *myosin heavy chain 4* (*Myh4*) in soleus muscles were determined by RT-qPCR, and 18S ribosomal RNA (18S rRNA) was used as an internal control; the relative *Myh1*, *Myh2*, and *Myh4* level was determined by the $2^{-\triangle\triangle}$CT. The primers used were as follows:

Myh1, forward primer 5'−3': GCGAATCGAGGCTCAGAACAA, reverse primer 5'−3': GTAGTTCCGCCTTCGGTCTTG;

Myh2, forward primer 5'−3': AAGTGACTGTGAAAACAGAAGCA, reverse primer 5'−3': GCAGCCATTTGTAAGGGTTGAC;

Myh4, forward primer 5'−3': CTTTGCTTACGTCAGTCAAGGT, reverse primer 5'−3': AGCGCCTGTGAGCTTGTAAA;

18S forward primer 5'−3': TCAAGAACGAAAGTCGGAGG, reverse primer 5'−3': GGACATCTAAGGGCATCAC.

2.10. pENN−AAV−U6−miR-29b overexpression vector

miR-29b overexpression vector pENN−AAV−U6−miR-29b was generated based on pENN-AAV-U6 plasmid. The forward and reverse primers of miR-29b were as follows: 5'−3': GATCTAGCACCA TTTGAAATCAGTGTTCTCGAGAACACTGATTTCAAATGGTGCTATTTTTG; 5'−3': AATTCAAAAATAGCACCATTTGAAATCAGTGTTCTCGAGAACACTGATTTCAAATGGTGCTA.

The 2 primers of miR-29b were denatured at 95°C for 10 min, annealed by gradually reducing the temperature and thus subcloned into pENN−AAV−U6 (BamHI and EcoRI double digestion). pENN−AAV−U6−miR29b was further verified by gene sequencing.

2.11. Adeno-associated virus serotype-8 (AAV8) packaging

The miR-29b overexpression construct (pENN-AAV-U6-miR-29b)/control plasmid (pENN-AAV-U6), packaging plasmids pAAV8 and pHelper were transfected into 293T using PEI, and AAV8 was packaged in 293T as described previously.[22] The AAV8 was purified by using iodixanol gradient density centrifugation.

2.12. Statistical analysis

All data in this study are reported as mean ± SD. Comparisons between the 2 groups were assessed by an independent sample *t* test. Comparisons among more than 2 groups were performed by a two-way analysis of variance (ANOVA) followed by the Tukey *post hoc* test. GraphPad Prism 8.0 software (GraphPad, San Diego, CA, USA) was used for the statistical analyses. Probability (*p* value) was used to indicate whether an observed difference is significant or occurred by random chance. A $p < 0.05$ was considered statistically significant.

3. Results

3.1. Exercise protects against AngII-induced muscle atrophy

We found that, based on the AngII-induced muscle-atrophy mouse model previously described,[18,19] treadmill running protected against AngII-induced muscle atrophy, as demonstrated by increased grip strength (Fig. 1A), the weight of the gastrocnemius (Fig. 1B) and tibialis anterior (Supplementary Fig. 1A), the cross-sectional area of myofiber (Fig. 1C and Supplementary Fig. 1B), and the area of myofiber (Fig. 1D and Supplementary Fig. 1C in both the gastrocnemius and the tibialis anterior.

Additionally, as further determined in the gastrocnemius based on the AngII-induced muscle atrophy model, treadmill running significantly decreased muscle atrogenes, including Atrogin-1 and MuRF-1 (Fig. 1E) and increased phosphorylation of AKT (S473), FOXO3A(S253), mTOR, p70 Ribosomal protein S6 Kinase (p70S6K), and eukaryotic initiation factor 4E (eIF-4E) binding protein 1 (EIF-4EBP1) (Fig. 1F). Apoptosis in skeletal muscles was also decreased by exercise, as demonstrated by decreased TUNEL-positive cells (Fig. 1G) and decreased ratios of B-cell lymphoma-2 (Bcl-2)-associated X (Bax)/B-cell lymphoma-2 (Bcl-2) and cleaved-cysteine-aspartic acid protease 3 (cleaved-caspase-3)/caspase-3 (Fig. 1H).

Furthermore, we found that the weight of the soleus, which is a typical slow-twitch fiber, was also increased by exercise (Supplementary Fig. 1D). In addition, the expression of *Myh2* (encoding myosin isoforms MyHC-IIa) was upregulated, whereas *Myh4* (encoding myosin isoforms MyHC-IIb) was downregulated in the soleus by exercise. *Myh1* was not obviously changed in the soleus by exercise (Supplementary Fig. 1E).

Collectively, these data suggest that exercise training can significantly attenuate muscle atrophy induced by AngII infusion.

3.2. Exercise upregulates PPARγ and downregulates miR-29b in AngII-induced muscle atrophy

We recently have reported that PPARγ was significantly decreased while miR-29b was increased in the AngII-induced muscle atrophy mice model.[18,19] In the present study, we found that treadmill running significantly upregulated PPARγ (Fig. 2A) and downregulated miR-29b (Fig. 2B) in the AngII-induced muscle atrophy model, suggesting that exercise might

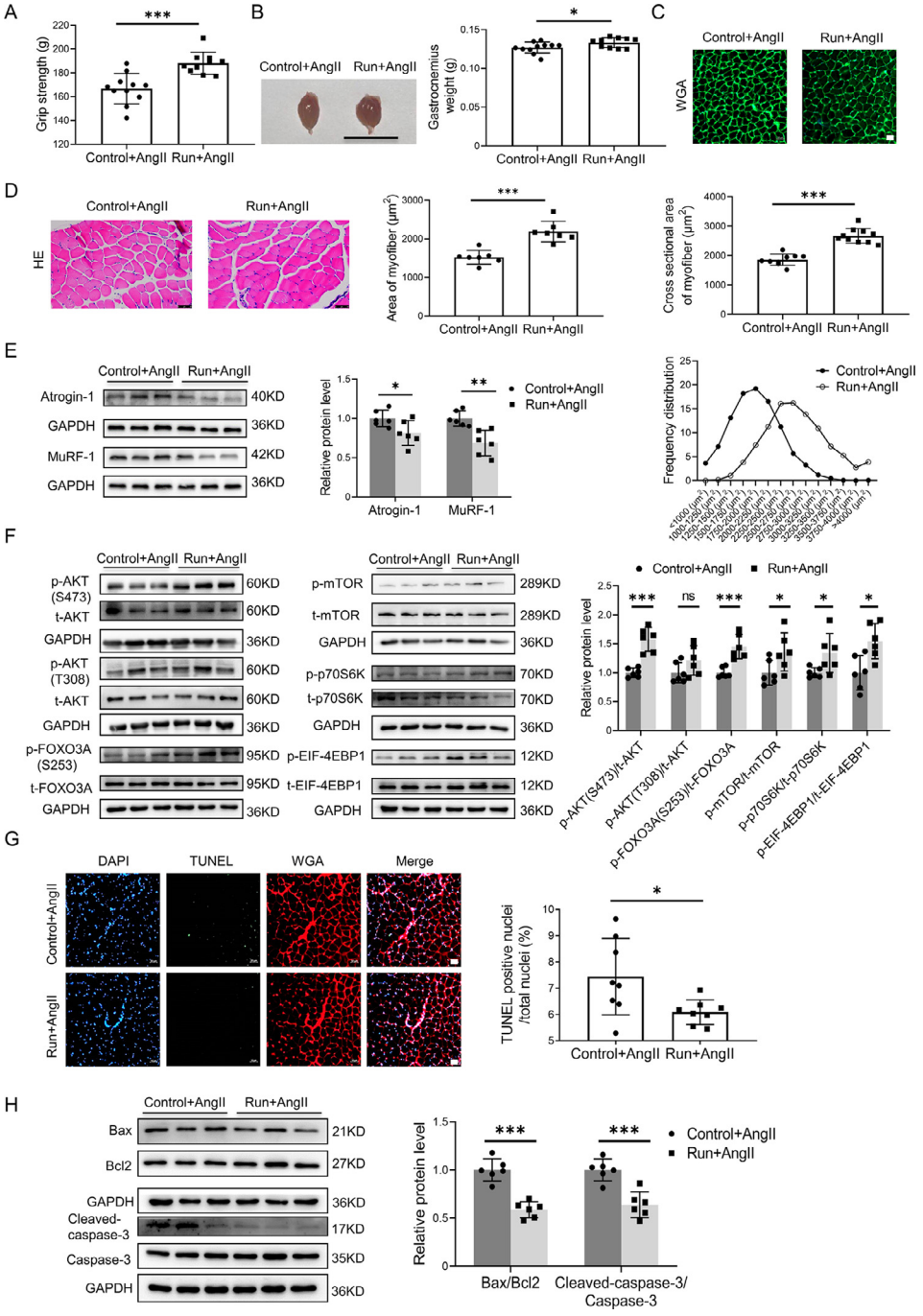

Fig. 1. Exercise protects against AngII-induced muscle atrophy. (A) The grip strength of mice in the Ang-infused control ($n = 11$) and run groups ($n = 10$) were evaluated. (B) Gastrocnemius was harvested from mice in the AngII-treated control and run groups, and muscle weight was measured; scale bar = 1 cm, $n = 11{:}10$. (C) The cross-sectional area of myofiber of gastrocnemius in the AngII-infused control and run groups was observed and measured by WGA staining, scale bar = 50 μm, $n = 9{:}10$. (D) The AngII-induced muscle atrophy of the gastrocnemius in the control and run groups was evaluated by HE staining, scale bar = 50 μm, $n = 7{:}7$. (E) The expression of Atrogin-1 and MuRF-1 in gastrocnemius in the AngII-infused control and run groups was detected by western blot; GAPDH was used as the loading control, $n = 6{:}6$. (F) Western blot was used to detect the phosphorylation of the AKT/FOXO3A/mTOR pathway proteins (AKT, FOXO3A, mTOR, p70S6K, and EIF-4EBP1) in the gastrocnemius in the AngII-infused control and run groups; GAPDH was used as the loading control, $n = 6{:}6$. (G) The apoptosis of the gastrocnemius in the AngII-infused control and run groups was detected by TUNEL staining. Blue indicates nuclear stained with DAPI, green indicates cells stained with TUNEL−FITC, and red indicates cell membrane stained with WGA conjugates, scale bar = 50 μm, $n = 8{:}8$. (H) The apoptosis-related proteins, including Bax, Bcl-2, cleaved caspase-3, and caspase-3, in the gastrocnemius in the AngII-infused control and run groups were detected by western blot; GAPDH was used as the loading control, $n = 6{:}6$. Data are presented as mean ± SD, each dot on the column indicates an independent sample in this group, and the number of dots on the column indicates the total number of samples in this group. Differences between the AngII-infused control and run groups were analyzed by an independent sample t test. * $p < 0.05$; ** $p < 0.01$; *** $p < 0.001$. AKT = protein kinase B; AngII = angiotensin II; Atogin-1 = F-box-only protein 32; BAX = Bcl-2-associated X; Bcl2 = B-cell lymphoma-2; Caspase-3 = cysteine-aspartic acid protease 3; DAPI = 4, 6-diamidino-2-phenylindole; EIF-4EBP1 = eukaryotic initiation factor 4E (EIF-4E) binding protein 1; FOXO3A = forkhead box O3A; GAPDH = glyceraldehyde-3-phosphate dehydrogenase; HE = Hematoxylin-eosin; mTOR = mammalian target of rapamycin; MuRF-1 = muscle specific RING-finger 1; ns = not significant; p70S6K = p70 ribosomal protein s6 kinase; p = phosphorylation; T = total; TUNEL = terminal deoxynucleotidyl transferase dUTP nick end labeling; TUNEL-FITC = TUNEL-fluorescein isothiocyanate; WGA = wheat germ agglutinin.

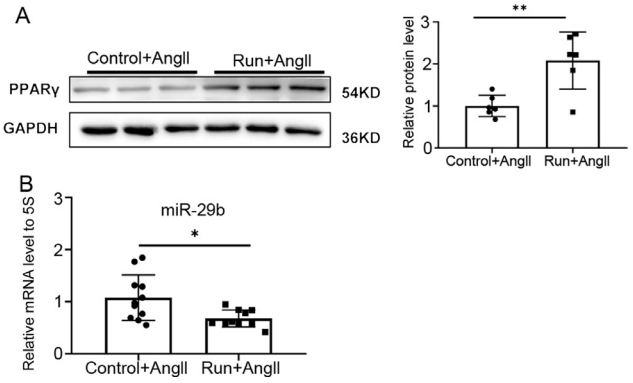

Fig. 2. Exercise upregulates PPARγ and downregulates miR-29b in AngII-induced muscle atrophy. (A) The expression of PPARγ in the gastrocnemius in the AngII-infused control ($n = 6$) and run groups ($n = 6$) was measured by western blot; GAPDH was used as the loading control. (B) The miR-29b expression level relative to 5S in the gastrocnemius in the AngII-infused control ($n = 11$) and run groups ($n = 10$) were detected by RT-qPCR. Data are presented as mean ± SD. Differences between the AngII-treated control and run groups were analyzed by an independent sample t test. * $p < 0.05$; ** $p < 0.01$. 5S = 5S ribosomal RNA; AngII = angiotensin II; GAPDH = glyceraldehyde-3-phosphate dehydrogenase; miR-29b = microRNA-29b; PPARγ = peroxisome proliferator-activated receptor gamma; RT-qPCR = reverse transcription quantitative polymerase chain reaction.

protect against AngII-induced muscle atrophy by increasing PPARγ and/or inhibiting miR-29b.

3.3. *The protective effects of exercise in AngII-induced muscle atrophy are negated by a PPARγ inhibitor*

To examine whether PPARγ activation is responsible for the beneficial effects of exercise training in AngII-induced muscle atrophy, a PPARγ inhibitor (T0070907) was intraperitoneally injected in both the AngII-infused control group and the run group of mice, while the other 2 parallel mouse groups were injected with solvent. T0070907 significantly reduced the expression of PPARγ in skeletal muscle cells (Fig. 3A) and reversed the protective effects of treadmill running in the AngII-induced muscle atrophy mice model, as demonstrated by decreased grip strength (Fig. 3B) and the weight of the gastrocnemius (Fig. 3C) and tibialis anterior (Supplementary Fig. 2A). Moreover, as further determined by the gastrocnemius, inhibition of PPARγ negated the protective effects of treadmill running in the AngII-induced muscle atrophy mouse model, as demonstrated by the decreased cross-sectional area of myofiber (Fig. 3D) and the area of the myofiber (Fig. 3E). PPARγ inhibitor increased muscle atrogenes, including the Atrogin-1 and MuRF-1 (Fig. 3F); decreased phosphorylation of AKT (S473), FOXO3A(S253), mTOR, p70S6K, and EIF-4EBP1 (Fig. 3G); and increased apoptosis as determined by TUNEL staining and western blot for the ratios of Bax/Bcl-2 and cleaved-caspase-3/caspase-3 (Figs. 3H and 3I). Furthermore, the muscle fiber types in the gastrocnemius were evaluated by immunostaining using specific antibodies of 3 myosin isoforms (myosin heavy chain type I antibody: BA-D5; myosin heavy chain type IIA antibody: SC-71; and myosin heavy chain type IIB antibody: BF-F3) and the corresponding fluorescent dye-conjugated secondary antibodies. We found that exercise regulated muscle fibers in the gastrocnemius in the same way that it did in the soleus, mainly through upregulating type IIA muscle fibers and downregulating type IIB muscle fibers. Moreover, we found that inhibition of PPARγ by T0070907 reduced exercise-triggered type IIA muscle fiber increase (Fig. S2B). Thus, PPARγ activation is essential for the beneficial effects of exercise in Ang-induced muscle atrophy.

3.4. *The protective effects of exercise in AngII-induced muscle atrophy are ameliorated by miR-29b overexpression*

To investigate whether miR-29b inhibition is responsible for the protective effects of exercise training in AngII-induced muscle atrophy, miR-29b overexpression adeno-associated virus serotype-8 (AAV8−miR-29b) or control AAV8 (AAV8-control) was injected into the gastrocnemius and tibialis anterior of the right hind limb of mice in both the control and the run groups. RT-qPCR analysis showed that miR-29b overexpression AAV8 significantly increased the expression of miR-29b in gastrocnemius (Supplementary Fig. 3A). AAV8-mediated miR-29b overexpression abolished the protective effects of treadmill running in the AngII-induced muscle atrophy mouse model, as demonstrated by the decreased grip strength (Fig. 4A) and the weight of the gastrocnemius and tibialis anterior (Fig. 4B and Supplementary Fig. 3B). Moreover, as further determined in the gastrocnemius, AAV8-mediated miR-29b overexpression ameliorated the protective effects of treadmill running in the AngII-induced muscle atrophy mouse model, as demonstrated by the decreased cross-sectional area of myofiber (Fig. 4C); the area of myofiber (Fig. 4D); upregulated muscle atrogenes, including Atrogin-1 and MuRF-1 (Fig. 4E); downregulated phosphorylation of AKT(S473), FOXO3A (S253), mTOR, p70S6K, and EIF-4EBP1 (Fig. 4F); and increased apoptosis (Fig. 4G). The composition of the muscle fiber types in the gastrocnemius were evaluated by immunostaining. Exercise upregulated type IIA muscle fiber and reduced type IIB muscle fiber, while overexpression of miR-29b inhibited exercise-triggered type IIA muscle fiber increase and type IIB decrease (Supplementary Fig. 3C). Therefore, miR-29b inhibition is required to achieve the beneficial effects of exercise in AngII-induced muscle atrophy.

4. Discussion

HF and muscle atrophy are mutually interacting clinical syndromes.[23,24] Muscle atrophy aggravates the adverse outcomes of chronic HF, increasing morbidity and mortality.[25] Exercise therapy currently represents the most commonly used and effective therapy for muscle atrophy.[9,10] However, patients with HF and muscle atrophy are characterized by decreased exercise capacity and may not be able to endure long periods of training.[3,4] Thus, it is important to investigate the key protective sensors of exercise as novel therapy targets for treatment of muscle atrophy.

In our study, we found that exercise protected AngII-induced muscle atrophy by targeting PPARγ/miR-29b (Fig. 5). The following facts support this finding. First, we

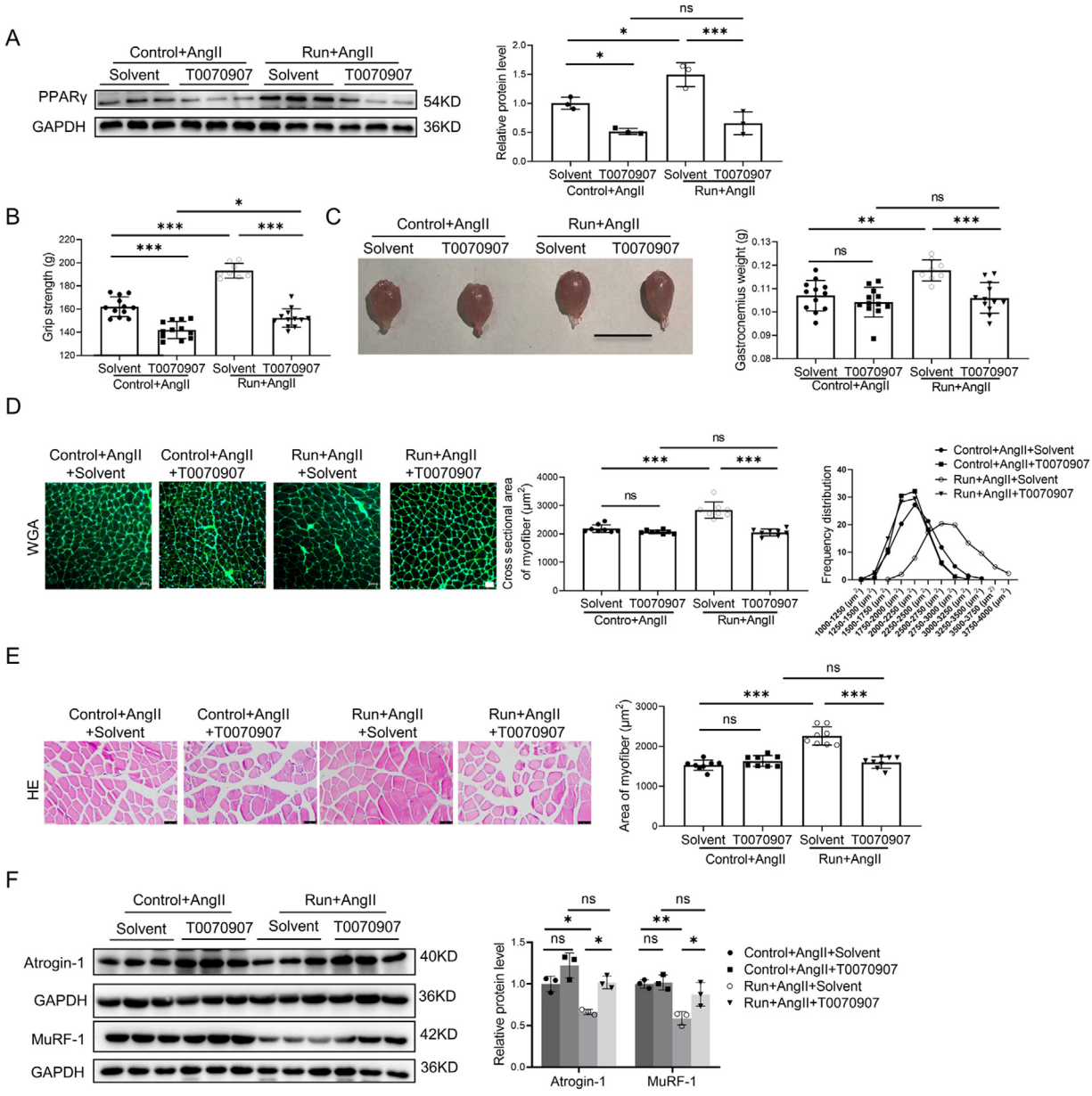

Fig. 3. The protective effect of exercise in AngII-induced muscle atrophy was abolished by a PPARγ inhibitor. (A) The expression of PPARγ in the gastrocnemius in the AngII-infused control and run groups, treated with or without the PPARγ inhibitor (T0070907), was measured by western blot; GAPDH was used as the loading control, $n = 3:3:3:3$. (B) The grip strength of mice in the AngII-infused control and run groups, treated with or without the PPARγ inhibitor (T0070907), was measured, $n = 12:12:8:12$. (C) The gastrocnemius was harvested from the AngII-infused control and run groups, treated with or without the PPARγ inhibitor (T0070907), and muscle weight was measured; scale bar = 1 cm, $n = 12:12:8:12$. (D) The cross-sectional area of myofiber of the gastrocnemius in the AngII-infused control and run groups, treated with or without the PPARγ inhibitor (T0070907), was measured by WGA staining, scale bar = 50 μm, $n = 8:8:8:8$. (E) The AngII-induced muscle atrophy of the gastrocnemius in the AngII-infused control and run groups, treated with or without the PPARγ inhibitor (T0070907), was evaluated by HE staining, scale bar = 50 μm, $n = 8:8:8:8$. (F) The expression of Atrogin-1 and Murf-1 in the gastrocnemius in the AngII-infused control and run groups, treated with or without PPARγ inhibitor (T0070907), was detected by western blot; GAPDH was used as the loading control, $n = 3:3:3:3$. (G) Western blot was used to detect the phosphorylation of the AKT/FOXO3A/mTOR pathway proteins (AKT, FOXO3A, mTOR, p70S6K, and EIF-4EBP1) in the gastrocnemius in the AngII-infused control and run groups, treated with or without the PPARγ inhibitor (T0070907); GAPDH was used as the loading control, $n = 3:3:3:3$. (H) The apoptosis of the gastrocnemius in the AngII-infused control and run groups, treated with or without the PPARγ inhibitor (T0070907), was observed by TUNEL staining: blue indicates nuclear stained with DAPI, green indicates cells stained with TUNEL-FITC, and red indicates cell membrane stained with WGA conjugates; scale bar = 50μm, $n = 8:8:8:7$. (I) Western blot was used to evaluate the apoptosis-related proteins, including Bax, Bcl-2, cleaved caspase-3, and caspase-3, in the gastrocnemius in the AngII-infused control and run groups, treated with or without the PPARγ inhibitor (T0070907); GAPDH was used as the loading control, $n = 3:3:3:3$. Results are presented as mean ± SD, each dot on the column indicates an independent sample in this group, and the number of dots on the column indicates the total number of samples in this group. Two-way ANOVA followed by the Tukey *post hoc* test was used to analyze the data. * $p < 0.05$; ** $p < 0.01$; *** $p < 0.001$. AKT = protein kinase B; AngII = angiotensin II; ANOVA = analysis of variance; Atrogin-1 = F-box only protein 32; BAX = Bcl-2-associated X; Bcl2 = B-cell lymphoma-2; Caspase-3 = cysteine-aspartic acid protease 3; DAPI = 4, 6-diamidino-2-phenylindole; EIF-4EBP1 = eukaryotic initiation factor 4E (eIF-4E) binding protein 1; FOXO3A = Forkhead box O3A; GAPDH = glyceraldehyde-3-phosphate dehydrogenase; mTOR = mammalian target of rapamycin; MuRF-1 = muscle specific RING-finger 1; ns = not significant; p70S6K = p70 ribosomal protein S6 kinase; p = phosphorylation; PPARγ = peroxisome proliferator-activated receptor gamma; TUNEL = terminal deoxynucleotidyl transferase dUTP nick end labeling; T = total; TUNEL-FITC = TUNEL-fluorescein isothiocyanate; WGA = wheat germ agglutinin.

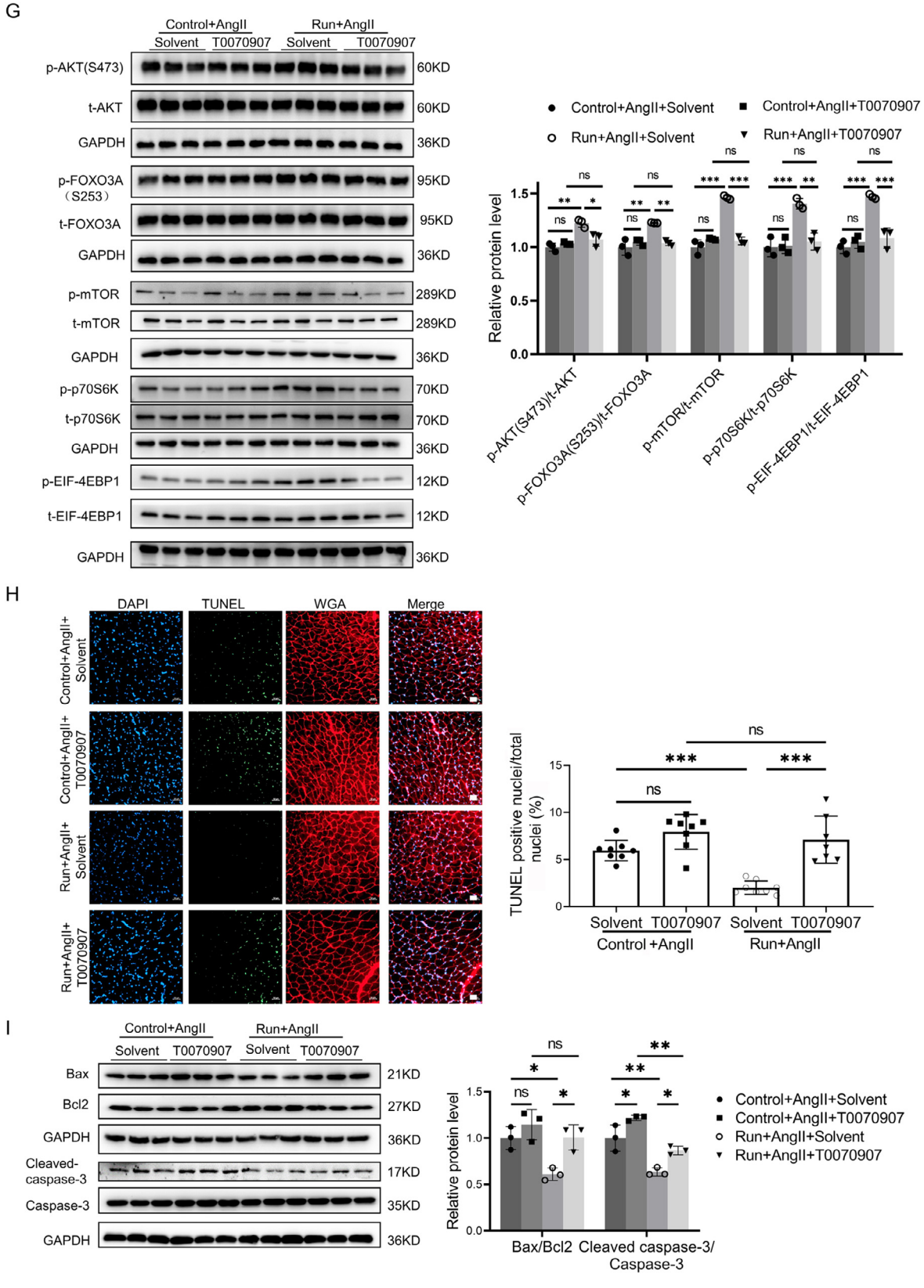

Fig. 3 Continued.

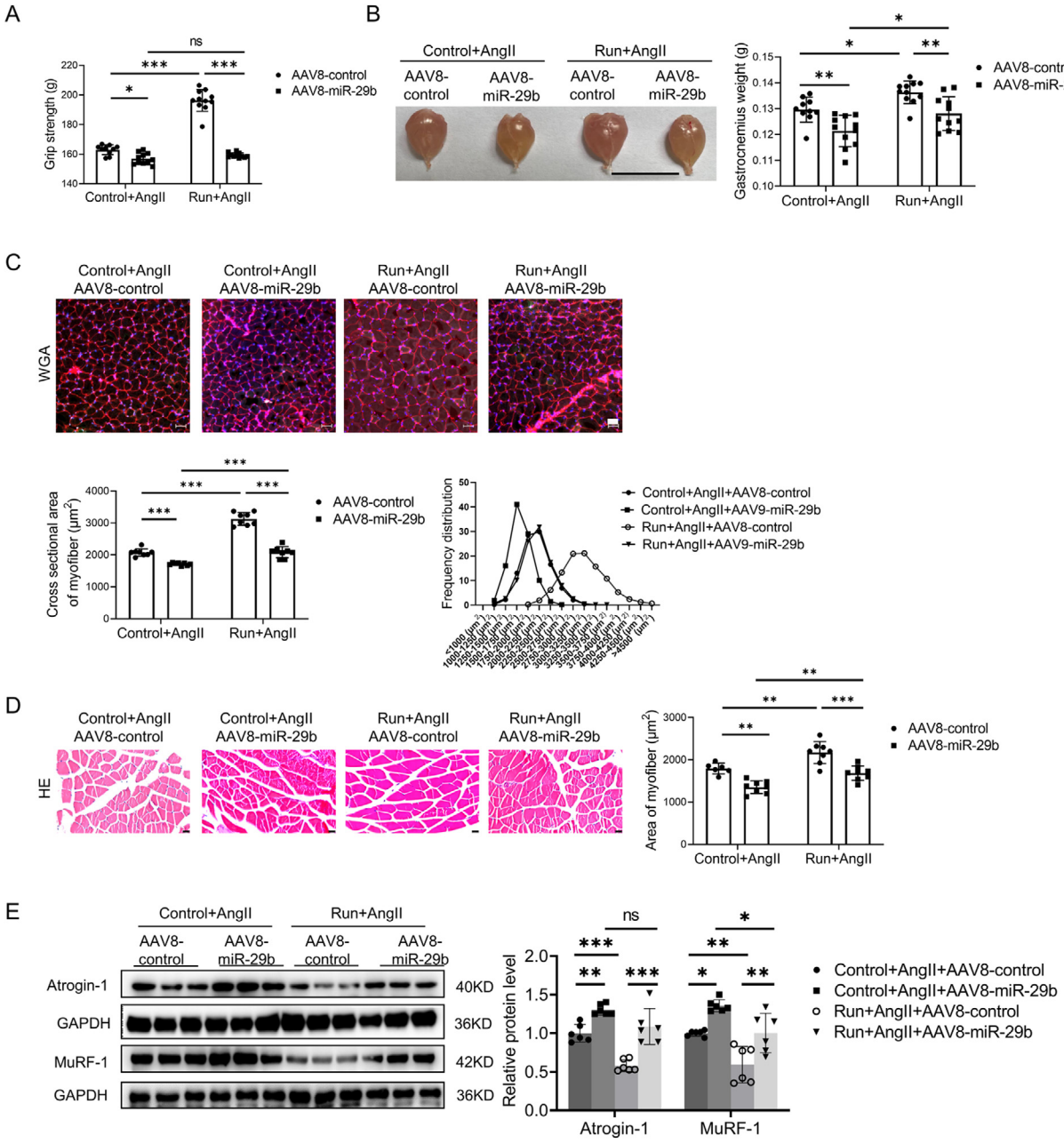

Fig. 4. The protective effect of exercise in AngII-induced muscle atrophy was abolished by miR-29b overexpression. (A) The grip strength of mice in the AngII-infused control and run groups, treated with control AAV8 (AAV8-control) or miR-29b overexpression AAV8 (AAV8-miR-29b) was measured, $n = 10:11:11:11$. (B) The gastrocnemius was harvested from mice of the AngII-infused control and run groups, treated with control AAV8 or miR-29b overexpression AAV8, and muscle weight was measured; scale bar = 1 cm, $n = 10:11:11:11$. (C) The cross-section area of myofiber of the gastrocnemius in the AngII-infused control and run groups, treated with control AAV8 or miR-29b overexpression AAV8, was measured by WGA staining; scale bar = 50 μm, $n = 8:8:8:8$. (D) The AngII-induced muscle atrophy of the gastrocnemius in the control and run groups, treated with control AAV8 or miR-29b overexpression AAV8, was evaluated by HE staining; scale bar = 50 μm, $n = 6:8:8:8$. (E) The expression of Atrogin-1 and MuRF-1 in the gastrocnemius in the AngII-infused control and run groups, treated with control AAV8 or miR-29b overexpression AAV8, was detected by western blot; GAPDH was used as the loading control, $n = 6:6:6:6$. (F) Western blot was used to detect the phosphorylation of AKT/FOXO3A/mTOR pathway proteins (AKT, FOXO3A, mTOR, P70S6K, and EIF-4EBP1) in the gastrocnemius in the AngII-infused control and run groups, treated with control AAV8 or miR-29b overexpression AAV8, GAPDH was used as the loading control, $n = 6:6:6:6$. (G) The AngII-induced apoptosis of the gastrocnemius in the control and run groups, treated with control AAV8 or miR-29b overexpression AAV8, was observed and measured by TUNEL staining; blue indicates nuclear stained with DAPI; green indicates cells stained with TUNEL-FITC; red indicates cell membrane stained with WGA conjugates); scale bar = 50 μm, $n = 8:8:8:8$. Results are presented as mean ± SD, each dot on the column indicates an independent sample in this group, and the number of dots on the column indicates the total number of samples in this group. Two-way ANOVA followed by the Tukey–*post hoc* text. AAV8 = adeno-associated virus serotype-8; AKT = protein kinase B; AngII = angiotensin II; ANOVA = analysis of variance; atogin-1 = F-box only protein 32; DAPI = 4, 6-diamidino-2-phenylindole; EIF-4EBP1 = eukaryotic initiation factor 4E (eIF-4E) binding protein 1; FOXO3A = Forkhead box O3A; GAPDH = glyceraldehyde-3-phosphate dehydrogenase; miR-29b = microRNA-29b; mTOR = mammalian target of rapamycin; MuRF-1 = muscle specific RING-finger 1; ns = not significant; p = phosphorylation; p70S6K = p70 ribosomal protein S6 Kinase; T = total; TUNEL = terminal deoxynucleotidyl transferase dUTP nick end labeling; TUNEL-FITC = TUNEL-fluorescein isothiocyanate; WGA = wheat germ agglutinin.

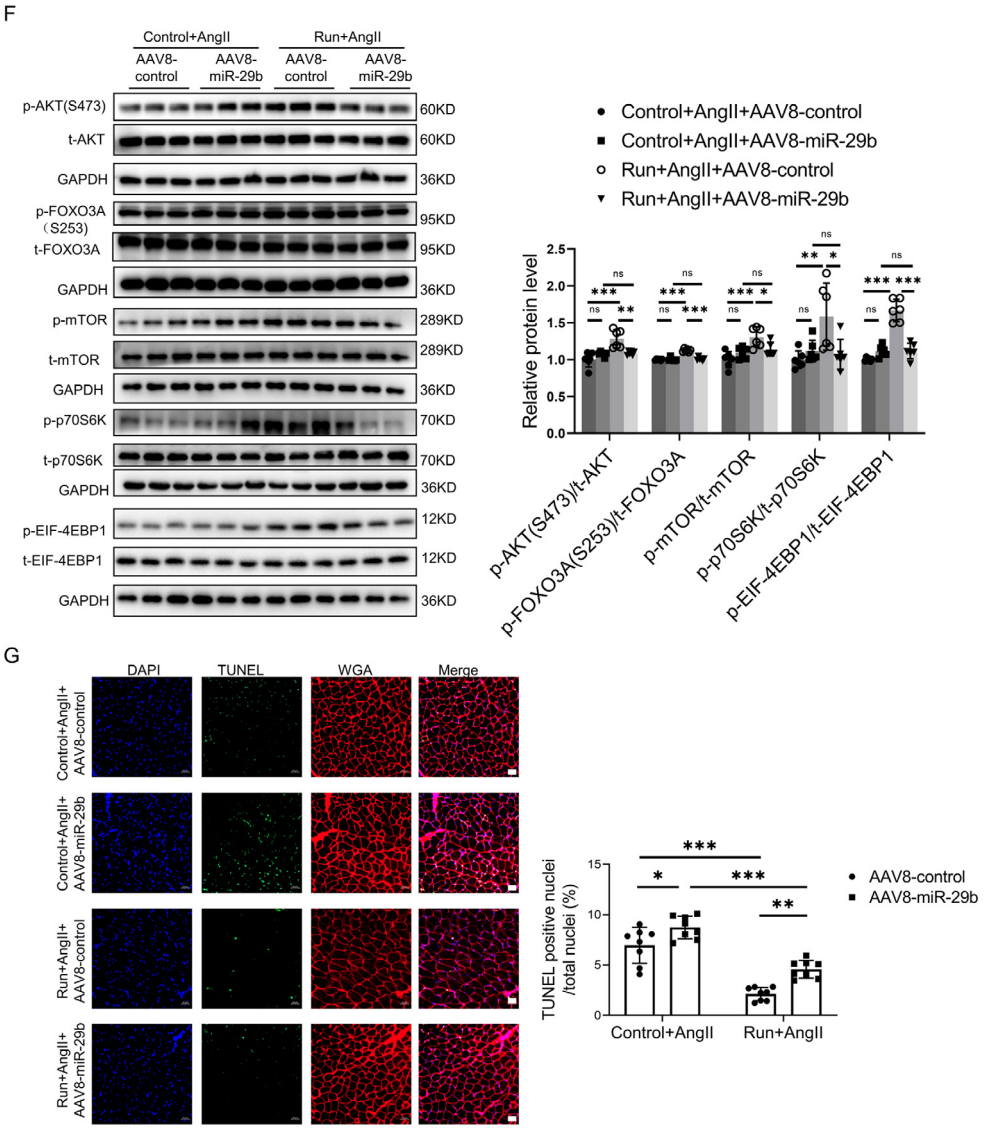

Fig. 4 Continued.

previously showed that PPARγ significantly decreased while miR-29b increased in the AngII-induced muscle atrophy mouse model.[18,19] We further found that exercise training significantly upregulated PPARγ and downregulated miR-29b in AngII-induced muscle atrophy. Second, the protective effects of exercise training in AngII-induced muscle atrophy was abolished by the PPARγ inhibitor, suggesting that PPARγ activation is necessary for the beneficial effects of exercise training in AngII-induced muscle atrophy. Third, the protective effects of exercise in AngII-induced muscle atrophy were ameliorated by miR-29b overexpression, suggesting that miR-29b inhibition mediates the protective effects of exercise training in AngII-induced muscle atrophy. Additionally, we found that miR-29b was significantly downregulated, while PPARγ was upregulated by exercise without AngII treatment (Supplementary Fig. 4), indicating that miR-29b and PPARγ are 2 important adaptive effectors of exercise in both physiological and pathological conditions (Fig. 2 and Supplementary Fig. 4). Collectively, these data confirm that exercise training protects AngII-induced muscle atrophy by targeting PPARγ/miR-29b.

PPARs, consisting of 3 family members (PPARα, PPARβ, and PPARγ) in skeletal muscles, are nuclear-receptor family

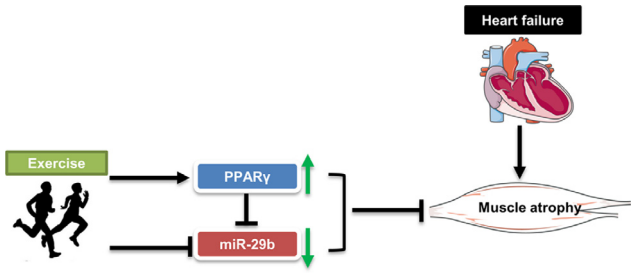

Fig. 5. The model of exercise-mediated protective function against AngII-induced muscle atrophy. miR-29b = microRNA-29b; PPARγ = peroxisome proliferator-activated receptor gamma.

transcription factors.[26] PPARs are involved in regulating genes that play a role in metabolism, energy production, inflammation, and many other cellular processes.[27] Muscle-specific knockout PPARγ mice showed an increase in adipose tissue mass, insulin resistance, and glucose intolerance.[28,29] Mice with overexpression of PPARγ in their skeletal muscle increased their adiponectin production and insulin sensitivity and decreased their myosteatosis.[30] Activation of PPARγ by using synthetic agonists in mice lacking PPARγ in their adipose tissues resulted in an increase in the insulin activity in their skeletal muscles and in their glucose use.[31] Recently, our group found that PPARγ played a critical role in AngII-induced muscle atrophy that inhibiting PPARγ-aggravated muscle atrophy while activating PPARγ-attenuated muscle atrophy.[19] Moreover, long-term administration of PPARγ agonists improved age-associated muscle mass loss and metabolism.[32] PPARγ has been reported to be activated by exercise;[33–35] however, whether PPARγ controls the beneficial effects of exercise in AngII-induced muscle atrophy is unknown. In our study, we provide direct evidence that PPARγ activation is required for the protective effects of exercise in AngII-induced muscle atrophy, suggesting that PPARγ is a key exercise-protective sensor.

Noncoding RNAs are involved in the regulation of many important physiological and pathological processes, including skeletal muscle development and muscle atrophy.[36,37] Our group has identified miR-29b as a common regulator of multiple types of muscle atrophy, including AngII-induced muscle atrophy.[18] Subsequently, we developed a clustered regularly interspaced short palindromic repeats (CRISP)/CRISPR-associated protein 9 (cas9)-mediated miR-29b editing system as a treatment for AngII-induced muscle atrophy in mice.[38] Additionally, we identified long noncoding RNA muscle atrophy associated transcript (MAAT) (lncMAAT) as a common regulator of muscle atrophy, which negatively regulates the transcription of miR-29b through sex determining region Y (SRY)-box 6 (SOX6) by a trans-regulatory module and upregulates its neighboring gene, muscle blind-like protein 1 (Mbnl1), by a cis-regulatory module.[39] Very recently, we identified miR-29b as a downstream target of PPARγ in AngII-induced muscle atrophy.[19] PPARγ can bind to the promoter region of miR-29b and negatively regulate miR-29b expression. In the present study, we found that when PPARγ expression was specifically inhibited by T0070907 in the run group, miR-29b was upregulated (Supplementary Fig. 2C). In addition, when miR-29b was overexpressed in the run group, PPARγ was downregulated (Supplementary Fig. 3D), indicating that PPARγ and miR-29b coordinately regulate the beneficial effects of exercise in AngII-induced muscle atrophy. Notably, in the present study we found that in the AngII-induced muscle atrophy mice model, PPARγ inhibition did not further aggravate muscle atrophy, while miR-29b overexpression further aggravated muscle atrophy, suggesting other upstream regulators of miR-29b exist. In heart tissues, exercise may increase miR-29.[40,41] However, how exercise regulates miR-29, especially miR-29b, in skeletal muscle is still undetermined. In the present study, we found that treadmill running decreased miR-29b in skeletal muscles and that miR-29b inhibition is necessary for the protective effects of exercise in AngII-induced muscle atrophy, suggesting that miR-29b, as a downstream target of PPARγ, is also an important exercise-protective sensor.

Compared to resistance exercise, aerobic exercise training has been assumed to have minimal impact on skeletal muscle mass. Treadmill running, compared to resistance exercise, has received little clinical or scientific inquiry regarding the treatment of muscle atrophy.[42,43] In our study, treadmill running, at a speed of 15 m/min for 60 min/day, was applied to the run group of mice. In addition, we added a 15° slope in order to increase resistance during exercise. We found that this treadmill running protocol was a useful, effective, and more easily performed method of preventing AngII-induced muscle atrophy in our mouse model. Our study provides further clinical evidence for combining aerobic- and resistance-exercise therapy in the treatment of muscle atrophy.

Acknowledgments

This work was supported by grants from the National Key Research and Development Project (2020YFA0803800 to JL, 2018YFE0113500 to JX), National Natural Science Foundation of China (82020108002 and 81911540486 to JX), Innovation Program of Shanghai Municipal Education Commission (2017-01-07-00-09-E00042 to JX), Science and Technology Commission of Shanghai Municipality (20DZ2255400 and 18410722200 to JX) and the "Dawn" Program of the Shanghai Education Commission (19SG34 to JX).

Authors' contributions

QL, LC, XL, YC, XZ, and SW contributed to acquisition of the data; JL, JG, and JX contributed to the design of the experiment. All authors contributed to the analysis of the data and to the writing of the manuscript. All authors have read and approved the final version of the manuscript, and agree with the order of presentation of the authors.

Competing interests

The authors declare that they have no competing interests.

Supplementary materials

Supplementary materials associated with this article can be found in the online version at doi:10.1016/j.jshs.2021.06.002.

References

1. Lavine KJ, Sierra OL. Skeletal muscle inflammation and atrophy in heart failure. *Heart Fail Rev* 2017;**22**:179–89.
2. Wood N, Straw S, Scalabrin M, Roberts LD, Witte KK, Bowen TS. Skeletal muscle atrophy in heart failure with diabetes: From molecular mechanisms to clinical evidence. *ESC Heart Fail* 2021;**8**:3–15.
3. Toth MJ, Gottlieb SS, Fisher ML, Poehlman ET. Skeletal muscle atrophy and peak oxygen consumption in heart failure. *Am J Cardiol* 1997;**79**:1267–9.
4. Mancini DM, Walter G, Reichek N, et al. Contribution of skeletal muscle atrophy to exercise intolerance and altered muscle metabolism in heart failure. *Circulation* 1992;**85**:1364–73.

5. Cabello-Verrugio C, Córdova G, Salas JD. AngiotensinII: Role in skeletal muscle atrophy. *Curr Protein Pept Sci* 2012;**13**:560–9.
6. Kadoguchi T, Kinugawa S, Takada S, et al. AngiotensinII can directly induce mitochondrial dysfunction, decrease oxidative fibre number and induce atrophy in mouse hindlimb skeletal muscle. *Exp Physiol* 2015;**100**:312–22.
7. Du Bois P, Pablo Tortola C, Lodka D, et al. AngiotensinII induces skeletal muscle atrophy by activating TFEB-mediated MuRF1 expression. *Circ Res* 2015;**117**:424–36.
8. Yin J, Lu X, Qian Z, Xu W, Zhou X. New insights into the pathogenesis and treatment of sarcopenia in chronic heart failure. *Theranostics* 2019;**9**:4019–29.
9. Liu Q, Gao J, Deng J, Xiao J. Current studies and future directions of exercise therapy for muscle atrophy induced by heart failure. *Front Cardiovasc Med* 2020;**7**:593429. doi:10.3389/fcvm.2020.593429.
10. Sartori R, Romanello V, Sandri M. Mechanisms of muscle atrophy and hypertrophy: Implications in health and disease. *Nat Commun* 2021;**12**:330. doi:10.1038/s41467-020-20123-1.
11. He N, Ye H. Exercise and muscle atrophy. *Adv Exp Med Biol* 2020;**1228**:255–67.
12. Souza RW, Piedade WP, Soares LC, et al. Aerobic exercise training prevents heart failure-induced skeletal muscle atrophy by anti-catabolic, but not anabolic actions. *PLoS One* 2014;**9**: e110020. doi:10.1371/journal.pone.0110020.
13. Cunha TF, Bacurau AV, Moreira JB, et al. Exercise training prevents oxidative stress and ubiquitin-proteasome system overactivity and reverse skeletal muscle atrophy in heart failure. *PLoS One* 2012;**7**:e41701. doi:10.1371/journal.pone.0041701.
14. Carvalho RF, Castan EP, Coelho CA, et al. Heart failure increases atrogin-1 and MuRF1 gene expression in skeletal muscle with fiber type-specific atrophy. *J Mol Histol* 2010;**41**:81–7.
15. Bodine SC, Baehr LM. Skeletal muscle atrophy and the E3 ubiquitin ligases MuRF1 and MAFbx/atrogin-1. *Am J Physiol Endocrinol Metab* 2014;**307**:E469–84.
16. Dalla Libera L, Ravara B, Volterrani M, et al. Beneficial effects of GH/IGF-1 on skeletal muscle atrophy and function in experimental heart failure. *Am J Physiol Cell Physiol* 2004;**286**:C138–44.
17. Yoshida T, Semprun-Prieto L, Sukhanov S, Delafontaine P. IGF-1 prevents ANGII-induced skeletal muscle atrophy via Akt- and Foxo-dependent inhibition of the ubiquitin ligase atrogin-1 expression. *Am J Physiol Heart Circ Physiol* 2010;**298**:H1565–70.
18. Li J, Chan MC, Yu Y, et al. miR-29b contributes to multiple types of muscle atrophy. *Nat Commun* 2017;**8**:15201. doi:10.1038/ncomms15201.
19. Li J, Yang T, Sha Z, et al. AngiotensinII-induced muscle atrophy via PPARγ suppression is mediated by miR-29b. *Mol Ther Nucleic Acids* 2020;**23**:743–56.
20. Smuder AJ, Morton AB, Hall SE, et al. Effects of exercise preconditioning and HSP72 on diaphragm muscle function during mechanical ventilation. *J Cachexia Sarcopenia Muscle* 2019;**10**:767–81.
21. Choe MA, Koo BS, An GJ, Jeon S. Effects of treadmill exercise on the recovery of dopaminergic neuron loss and muscle atrophy in the 6-ohda lesioned Parkinson's disease rat model. *Korean J Physiol Pharmacol* 2012;**16**:305–12.
22. Wei Y, Chen Y, Qiu Y, et al. Prevention of muscle wasting by CRISPR/Cas9-mediated disruption of myostatin *in vivo*. *Mol Ther* 2016;**24**: 1889–91.
23. Curcio F, Testa G, Liguori I, et al. Sarcopenia and heart failure. *Nutrients* 2020;**12**:211. doi:10.3390/nu12010211.
24. Suzuki T, Palus S, Springer J. Skeletal muscle wasting in chronic heart failure. *ESC Heart Fail* 2018;**5**:1099–107.
25. von Haehling S. The wasting continuum in heart failure: From sarcopenia to cachexia. *Proc Nutr Soc* 2015;**74**:367–77.
26. Manickam R, Duszka K, Wahli W. PPARs and microbiota in skeletal muscle health and wasting. *Int J Mol Sci* 2020;**21**:8056. doi:10.3390/ijms21218056.
27. Benton CR, Koonen DP, Calles-Escandon J, et al. Differential effects of contraction and PPAR agonists on the expression of fatty acid transporters in rat skeletal muscle. *J Physiol* 2006;**573**:199–210.
28. Hevener AL, He W, Barak Y, et al. Muscle-specific Pparg deletion causes insulin resistance. *Nat Med* 2003;**9**:1491–7.
29. Norris AW, Chen L, Fisher SJ, et al. Muscle-specific PPARgamma-deficient mice develop increased adiposity and insulin resistance but respond to thiazolidinediones. *J Clin Invest* 2003;**112**:608–18.
30. Amin RH, Mathews ST, Camp HS, Ding L, Leff T. Selective activation of PPARgamma in skeletal muscle induces endogenous production of adiponectin and protects mice from diet-induced insulin resistance. *Am J Physiol Endocrinol Metab* 2010;**298**:E28–37.
31. He W, Barak Y, Hevener A, et al. Adipose-specific peroxisome proliferator-activated receptor gamma knockout causes insulin resistance in fat and liver but not in muscle. *Proc Natl Acad Sci U S A* 2003;**100**:15712–7.
32. Xu L, Ma X, Verma N, et al. PPARγ agonists delay age-associated metabolic disease and extend longevity. *Aging Cell* 2020;**19**:e13267. doi:10.1111/acel.13267.
33. Zheng F, Cai Y. Concurrent exercise improves insulin resistance and non-alcoholic fatty liver disease by upregulating PPAR-γ and genes involved in the beta-oxidation of fatty acids in ApoE-KO mice fed a high-fat diet. *Lipids Health Dis* 2019;**18**:6. doi:10.1186/s12944-018-0933-z.
34. Ruffino JS, Davies NA, Morris K, et al. Moderate-intensity exercise alters markers of alternative activation in circulating monocytes in females: A putative role for PPARγ. *Eur J Appl Physiol* 2016;**116**:1671–82.
35. Thomas AW, Davies NA, Moir H, et al. Exercise-associated generation of PPARγ ligands activates PPARγ signaling events and upregulates genes related to lipid metabolism. *J Appl Physiol (1985)* 2012;**112**:806–15.
36. Chen R, Lei S, Jiang T, She Y, Shi H. Regulation of skeletal muscle atrophy in cachexia by microRNAs and long non-coding RNAs. *Front Cell Dev Biol* 2020;**8**:577010. doi:10.3389/fcell.2020.577010.
37. Li Y, Meng X, Li G, Zhou Q, Xiao J. Noncoding RNAs in muscle atrophy. *Adv Exp Med Biol* 2018;**1088**:249–66.
38. Li J, Wang L, Hua X, et al. CRISPR/Cas9-mediated miR-29b editing as a treatment of different types of muscle atrophy in mice. *Mol Ther* 2020;**28**:1359–72.
39. Li J, Yang T, Tang H, et al. Inhibition of LncRNA MAAT controls multiple types of muscle atrophy by cis- and trans-regulatory actions. *Mol Ther* 2021;**29**:1102–19.
40. Soci UP, Fernandes T, Hashimoto NY, et al. microRNAs 29 are involved in the improvement of ventricular compliance promoted by aerobic exercise training in rats. *Physiol Genomics* 2011;**43**:665–73.
41. Habibi P, Alihemmatti A, Alipour M, et al. Effects of exercise on miR-29 and IGF-1 expression and lipid profile in the heart of ovariectomized rat. *Acta Endocrinol (Buchar)* 2016;**12**:130–6.
42. Konopka AR, Harber MP. Skeletal muscle hypertrophy after aerobic exercise training. *Exerc Sport Sci Rev* 2014;**42**:53–61.
43. Wackerhage H, Schoenfeld BJ, Hamilton DL, Lehti M, Hulmi JJ. Stimuli and sensors that initiate skeletal muscle hypertrophy following resistance exercise. *J Appl Physiol (1985)* 2019;**126**:30–43.